PCL Scaffold Combined with Rat Tail Collagen Type I to Reduce Keratocyte Differentiation and Prevent Corneal Stroma Fibrosis after Injury.

Wenhan Xu
Huazhong University of Science and Technology Tongji Medical College First Clinical College: Wuhan Union Hospital
Bin Kong
Tsinghua University Graduate School at Shengzhen
Huatao Xie
Huazhong University of Science and Technology Tongji Medical College First Clinical College: Wuhan Union Hospital
Weijian Liu
Huazhong University of Science and Technology Tongji Medical College First Clinical College: Wuhan Union Hospital
Sheng Liu
Huazhong University of Science and Technology Tongji Medical College First Clinical College: Wuhan Union Hospital
Yanbin Zhang
Huazhong University of Science and Technology Tongji Medical College First Clinical College: Wuhan Union Hospital
Fan Yang
Huazhong University of Science and Technology Tongji Medical College First Clinical College: Wuhan Union Hospital
Jiheng Xiao
Huazhong University of Science and Technology Tongji Medical College First Clinical College: Wuhan Union Hospital
Jiaqi Zhang
Wuhan University of Science and Technology
Shengli Mi
Tsinghua University Graduate School at Shengzhen
Liming Xiong
Huazhong University of Science and Technology Tongji Medical College First Clinical College: Wuhan Union Hospital
Mingchang Zhang

Huazhong University of Science and Technology Tongji Medical College First Clinical College: Wuhan Union Hospital

Fagang Jiang (13554100999@163.com)

Huazhong University of Science and Technology Tongji Medical College First Clinical College: Wuhan Union Hospital https://orcid.org/0000-0002-7198-9085

Research

Keywords: corneal stroma injury, corneal fibrosis, keratocyte differentiation, corneal tissue engineering, near-field electrospinning

Posted Date: June 18th, 2021

DOI: https://doi.org/10.21203/rs.3.rs-626795/v1

Abstract

The cornea is one of the major refractive eye components with significant functions, and its transparency is essential for clear vision. With regard to corneal injury, the corneal epithelium has a strong self-healing ability, while the corneal stroma is not capable of total self-repair. Therefore, preventing fibrosis and reducing keratocyte differentiation after injury have always been a challenge. The severe shortage of donor corneas for transplantation and transplant rejection prompted the development of corneal tissue engineering. In this study, we fabricated a poly(ε-caprolactone) (PCL) microfibrous scaffold and infused the scaffold with rat tail collagen type I to obtain a 3D composite material. The PCL/collagen scaffold was designed to fabricate an optimal construct that simulates the stromal structure with properties that are most similar to the native cornea. The PCL scaffold has good mechanical properties, and infusion with rat tail collagen type I improved its biocompatibility. The results demonstrate that 3D composite material could reduce keratocyte differentiation, help achieve regular collagen distribution, and promote corneal repair.

1. Introduction

The cornea is a dome-shaped transparent tissue that functions as an optical lens that provides indispensable features to the visual system, including optical transparency and light refraction [1, 2]. Meanwhile, the cornea is exposed to a constantly changing external environment as the outermost layer of the eye and is thus most likely to sustain damage; there are more than 1.52 million new cases of corneal blindness reported for each year [3], of which only less than 5% of patients have opportunities for corneal transplantation due to severe shortage of donor cornea and the high cost of transplantation surgery [4, 5]. In terms of corneal injury, the corneal epithelium has a strong self-healing ability, whereas the corneal stroma may incur permanent corneal damage, leading to corneal stromal fibrosis and loss of vision [6]. Corneal transplantation has been the dominant procedure for more than 50 years, which highly depends on the availability of donor cornea [7]. Keratoprosthesis such as decellularized animal and human amniotic membrane transplant is associated with a lifetime risk of rejection [8, 9].

To meet the demand for corneal transplantation, diverse bioengineering methods have been attempted to fabricate corneal substitutes based on synthetic (e.g., perfluoropolyether (PFPE) [10], poly(vinyl alcohol) (PVA) [11, 12], poly(ε-caprolactone) (PCL) [13, 14], poly(methyl methacrylate) (PMMA) [15], poly(ethylene glycol) (PEG) [16], poly(hydroxyethyl methacrylate) (PHEMA) [17]or natural (e.g., silk [18], collagen [19, 20], amniotic membranes [21], gelatin [17]) materials [22, 23]. Furthermore, a combination of two or more synthetic and natural materials has been developed using 3D printing [24], electrospinning [13, 17], and hydrogels [25]. The corneal stroma is the most central tissue of the cornea, making up two-thirds of its structure and accounting for about 90% of the corneal mass and thickness of the cornea [13]. The regular arrangement of collagen in the corneal stroma is fundamental to the transparency of the cornea; when the cornea is injured, quiescent keratocytes can be activated and transformed into fibroblasts and myofibroblasts, which can secrete a large number of collagen fibers randomly to repair damage, rendering the repair of corneal stroma damage difficult [26, 27]. Therefore, the construction of a material

that simulates the orthogonally aligned fibrous structure of the corneal stroma is expected to make new progress in corneal bioengineering.

PCL is a synthetic polymer that is widely used in the preparation of scaffold materials mainly because it is viscoelastic, ductile, isomer-free, and low-cost. In addition, PCL shows a certain degree of biocompatibility, long-term biodegradability, and absorbability [28, 29]. It has been reported that the topological structure of a PCL fiber-reinforced GelMA hydrogel can maintain the keratocyte phenotype and induce cell differentiation [30]. Studies have also shown that PCL scaffolds produced by electrospinning can be used to culture breast cancer cells in vitro [31]. These properties make PCL a good option for biological tissue engineering.

The PCL polymer is dissolved, and the solution is charged at a high voltage. When the electricity overcomes the surface tension, the polymer solution is pulled onto the target plate, and the solvent is evaporated to collect intersecting nanofibers [32]. The structure mimics the stromal cell fiber assemblage in vitro, and the cultured cells can take on a shape similar to that in vivo [33, 34]. However, owing to the limitations of electrospinning in precisely controlling the network structure, the cells inoculated on the surface of the fibers cannot migrate to the internal structure [35]. With the development of science and technology, near-field electrospinning (NFES) was designed to overcome the intrinsic instability of traditional electrospinning processes and promote the controllable deposition of nanofibers under the action of a reduced electric field [36]. NFES or direct writing [37] can realize the hierarchical assembly and precise control of the network structure of sub-microscale fibers [38]. Advances in technology have raised the prospect of making an alternative that more closely resembles a native cornea.

The corneal stroma is principally composed of aligned collagen type I fibrils principally [26]. Collagen, as a natural biopolymer, is widely used in biomaterials in the medical field owing to its superior biocompatibility, biodegradability, and biological activity [39-41]. However, its poor mechanical properties limit its application in tissue engineering. Therefore, collagen is often used in conjunction with other materials to obtain mechanical support. Consequently, composite corneal grafts that possess mechanical properties and biocompatibility concurrently emerged [39, 42, 43]. The aforementioned PCL is an optimal choice. The PCL-collagen composite structure is applied not only in corneal tissue bioengineering but also in cartilage tissue engineering [41, 44], heart valve tissue engineering [40], Achilles t5tendon repair [43], long-segment tracheal replacement [42], bone repair [45], and wound care [46]. The construct can simulate the complex corneal stroma better and supply a 3D environment for cell growth, providing a mechanical basis for cells to adhere, migrate, and proliferate, while collagen affords a suitable growth environment.

A synthetic substance is combined with a natural substance in order to complement the deficiencies of PCL and collagen and make full use of their advantages at the same time. In this study, we fabricated a multilaminate orthogonally aligned PCL scaffold precisely by NFES, which was perfused by collagen to form a 3D corneal graft. We selected the optimal composite scaffold by measuring the mechanical strength, light transmittance, water content, swelling ratio, biocompatibility, and topological structures. In

vivo tests were conducted using a rat corneal stroma defect model to examine the fibrosis and regeneration of the corneal stroma after injury. Ultimately, we demonstrated that the designed composite scaffold has excellent mechanical and biological properties, which can reduce keratocyte differentiation and prevent corneal stroma fibrosis after injury.

2. Material And Methods

The materials and methods used in the study are detailed in the Supplementary materials and methods.

3. Results And Discussion

3.1 Fabrication of PCL/collagen scaffold. The PCL polymer was successfully used to fabricate the multilaminate orthogonally aligned scaffold by direct writing. Figure 1A and B show the actual and schematic representations of the direct writing equipment and the Taylor cone. In the process of direct writing, the formation speed of the jet and the movement velocity of the collector played an important role in controlling the morphology of the deposited fibers. In our previously study [30], we found that a stable PCL jet was obtained under the following conditions: 3.6-kV electrostatic voltage, 20-kPa gas pressure, 3-mm distance between the syringe needle and the collector plate, and a velocity of 60 mm/s. The grid scaffold was fabricated using a fiber spacing of 200 μm and stacked with 10 layers. Many studies have reported the printing of PCL scaffolds by electrospinning technology; however, owing to the poor control of the prepared fibers, only few studies fabricated orthogonally aligned scaffolds that successfully resembled the corneal stroma. They simply used PCL scaffolds as a mechanical support for corneal substitutes without a particular structure to simulate the corneal stroma [39, 47, 48]. It is difficult to control the pattern of PCL fibers precisely by electrospinning; more importantly, the electrospun fibers have low transmittance because of their high density, which makes them unsuitable as corneal substitutes. The NFES technique is a new electrospinning technology developed based on traditional methods to improve the control of fibers [49, 50]. PCL has a low melting temperature and stability, making it the most commonly used material in direct writing. However, PCL is less biocompatible, which limits its application in corneal bioengineering. Thus, we improved the biocompatibility of the PCL scaffold by infusing rat tail collagen type I.

The sterile rat tail collagen type I stock solution was neutralized with (NaOH 0.1M) to obtain a usable collagen solution at various concentrations (Figure 1C). The concentration of 3 mg/ml was too low to gelatinize, while that of 5 mg/ml and 8 mg/ml was adequate for gelatinization (Figure 1D). The PCL scaffold was fabricated by infusing collagen at concentrations of 3, 5, and 8 mg/ml mg (Figure 1E). We cut the rectangular scaffold with a 3.25-mm-diameter trephine to obtain a corneal graft (Figure 1F). Finally, we prepared the PCL scaffold and PCL/collagen scaffold for corneal transplantation (Figure 1G). During the preparation process, collagen perfusion at a concentration of 3 mg/ml was unable to completely facilitate gelatinization, while collagen perfusion with a concentration of 8 mg/ml did not completely fill the interspace of the PCL scaffold due to its high concentration and poor fluidity, resulting in uneven PCL/collagen scaffolds. For these aforementioned reasons, collagen at a concentration of 5

mg/ml was selected for perfusion. Orthogonally aligned PCL scaffolds infused with rat tail collagen type I were fabricated to simulate the native corneal stromal lamellae, which were first used in corneal tissue bioengineering.

3.2 Macroscopic and microscopic morphology characteristics of the PCL/collagen scaffold. The design of the corneal stroma structure is pivotal to repair defects in the anterior corneal lamina due to its special structure. In this study, we constructed a PCL/collagen scaffold to simulate the complex orthogonal lamellar structure of the corneal stroma. It consists of a synthetic PCL scaffold and natural rat tail collagen, which complement each other mechanically and biologically. The morphology of the PCL fibers and the deposition accuracy were observed by SEM at various magnifications (Figure 2A). The PCL fibers showed high deposition accuracy, with an average diameter of approximately 5μm. Horizontal and vertical printing constitutes one layer, stacking 10 layers of printing, making it 100 μm thick. Rat tail collagen has a loose and porous microstructure under SEM, which can provide a suitable growth environment for cells (Figure 2B). The PCL scaffold was filled with collagen homogeneously without affecting the lamellar structure of the PCL scaffold, as observed by SEM (Figure 2C). The collagen fibers of the corneal stroma have a special orthogonal lamellar structure; however, the collagen secreted after injury is disorganized without its original structure, resulting in the difficulty of completely repairing the corneal stroma. Some studies have also fabricated aligned fibers, but they are only partially aligned [48, 51]. The purpose of this grid-like PCL/collagen scaffold is to simulate the orthogonal lamellar structure of the native cornea to guide the regular arrangement of collagen fibers after injury and repair the corneal stromal injury.

3.3 Physical characterization of the PCL/collagen scaffold. Transparency is essential for corneal transplant function and is associated with collagen tissue concentration, which contributes to transparency through its water-retaining proteoglycan [52]. The light transmittance of the cornea, collagen, and scaffolds were determined using a spectrophotometer at wavelengths ranging from 400 to 800 nm (Figure 2D). Collagen at a concentration of 5 mg/ml and cornea had similar absorption curves in the visible light range, where the absorbance increased with increasing wavelength. The transparency of the cornea was approximately 87% [53], while that of collagen (64.74±8.11%) was lower than that of the cornea (87.77±6.19%) at 800 nm. The PCL scaffold with a fiber spacing of 200 μm had a higher light transmittance (90.67±1.08%) than that of the cornea, but its light transmittance decreased upon collagen infusion. The wet PCL/collagen scaffold has a higher transmittance than the dry one owing to the hydroscopicity of collagen. As the water content of the graft increased, the transmittance increased correspondingly.

As mentioned previously, the cornea is a transparent water-containing tissue with the ability to moisturize; thus, the water adsorption and swelling properties of corneal substitutes play an important role in maintaining the structural stability of the corneal graft, which facilitates cell migration, adhesion, and proliferation, and delivers nutrients to the corneal cells. To further evaluate the physical properties of the scaffolds, the water content and swelling ratio were determined to identify the hydrophilic properties of the materials. In our study, the water content of the PCL/collagen scaffold with a collagen concentration

of 5 mg/ml (85.26±0.94%) was not significantly different from that of the cornea (84.54±0.58%) (Figure 2G). Furthermore, the swelling ratios of the PCL/collagen scaffold at various concentrations and the cornea were measured under the same conditions (Figure 2H). No significant difference was observed in the swelling ratios of the cornea (32.66±2.29%) and PCL/collagen scaffolds with collagen at concentrations of 3 mg/ml (35.08±2.35%) and 5 mg/ml (31.12±0.61%). The water-uptake capability of the PCL/collagen scaffold with a collagen concentration of 5 mg/ml is similar to that of the native cornea, rendering it capable of meeting the requirement for use as a corneal substitute.

In addition to the transmittance and hydrophilicity of the PCL/collagen scaffold, the mechanical properties of the scaffold also play an important role in surgical suturing. Corneal substitutes require mechanical strength similar to that of native corneas or even higher in order to withstand the tension of the suture during surgery and the intraocular pressure after surgery. The tensile strain–stress curves and the maximum tensile strengths of the PCL scaffold, PCL/collagen scaffold, and rat cornea were measured. As shown in Figure 2E, the PCL scaffold had a higher elongation at break, which indicated that the ductility of PCL was higher than that of the native cornea. The elongation at break of the PCL/collagen scaffold and the native cornea was similar. The PCL scaffold and PCL/collagen scaffold attained the tensile strength requirements of the native cornea (2.06±0.16 MPa), with the maximum levels at 2.70±0.32 and 3.46±0.34 MPa, respectively (Figure 2F). The results showed that the PCL/collagen scaffold was able to exhibit adequate mechanical strength to withstand both the surgical suture and intraocular pressure, which was mainly due to the mechanical properties of PCL itself, and this was enhanced by collagen infusion.

The mechanical strength, light transmittance, swelling ratio, and water content should be considered as design criteria in the development of corneal substitutes, as these characteristics are crucial to the cornea. Thus, we measured the characteristics of PCL scaffolds infused with collagen at concentrations of 3 mg/ml, 5 mg/ml, and 8 mg/ml to identify the optimal design for PCL/collagen scaffolds. As shown in Figure 2D, the light transmittance of the PCL scaffold was reduced by the infusion of collagen, but it could still conform to the requirement of the native cornea. From the results shown in Figure 2E and F, the maximum tensile strength of the PCL scaffolds was improved by collagen perfusion and was higher than that of the native corneas, meeting the requirement for suturing during surgery. Figure 2G and H show the hydrophilicity of the scaffolds, and we found that the water content and swelling ratio were inversely proportional to the collagen concentration. A higher concentration implies less space, limiting the storage and absorption of water.

3.4 Cell proliferation and adhesion properties of the PCL/collagen scaffold in vitro. Corneal substitutes require good mechanical properties and biocompatibility with no cytotoxicity. They should also permit cells of the injured tissue to adhere and migrate into the scaffold for injury repair and integration. Thus, cell adhesion and proliferation assays were performed on the scaffolds. In this study, we obtained limbal stromal stem cells (LSSCs) from the rat limbus, which can proliferate rapidly in vitro, and a Cell Counting Kit-8 (CCK-8) kit was used to quantitatively estimate the adhesion and proliferation of LSSCs (Figure 3A). We selected the Matrigel commonly used in cell culture as the control group, and rat tail collagen with

concentrations of 3, 5, and 8 mg/ml were used as the experimental groups. In CCK-8 experiments, the proliferation rates of LSSCs on the four plates were close to each other at 1 day of culturing, and there were no significant differences. The proliferation rates increased with incubation time, with the exception of collagen at a concentration of 8 mg/ml (Supplementary Figure S1). The proliferation rate in collagen with a concentration of 3 mg/ml was the closest to that in Matrigel regardless of culture time, followed by a concentration of 5 mg/ml. The proliferation rates in collagen at a concentration of 5 mg/ml showed no significant differences compared to that in Matrigel at 1, 3, and 5 days of culturing. It can be concluded that natural rat tail collagen is non-cytotoxic and can provide a good environment for LSSC proliferation; thus, the concentrations of 3 and 5 mg/ml of collagen were optimal.

The proliferation rates of LSSCs cultured in the PCL scaffold, collagen, and the PCL/collagen scaffold were also estimated (Figure 3B). We observed that the proliferation rates of LSSCs on the three plates showed no significant differences after culturing for 1 day. The proliferation rates increased with the prolongation of culture time. The proliferation rate of LSSCs cultured in PCL scaffold was lower than that of the others, and the longer the culturing time, the more significant the differences were (Supplementary Figure S2). We speculated that the special structure of the PCL scaffold restricted the rapid growth of cells to some extent; it took longer for the cells to adhere and migrate to the regular PCL fibers and proliferate along the fibers. According to the differentiation of LSSCs and secretion of collagen after injury, the inhibition of cell proliferation may not be a disadvantage for injury repair.

The PCL/collagen scaffold provides more mechanical support, and the orthogonally arranged lamellar structure mimics the native corneal stroma and aims to guide the regular distribution of cells involved in repair and collagen secreted by fibroblasts and myofibroblasts after injury to reduce fibrosis. Immunofluorescence staining was used to observe the distribution of LSSCs on the PCL/collagen scaffold and on rat tail collagen without the PCL scaffold. LSSCs grew freely in collagen without specific rules and with high cell density (Figure 3C), while the cells grew along the two directions of PCL fibers and were distributed on different layers on the PCL/collagen scaffold (Figure 3D, E). In addition, the gap between the PCL fibers provided ample space for cell growth.

In the scaffolds we fabricated, the concentration of collagen was found to affect the proliferation rates of LSSCs. At the same time, we confirmed that 5 mg/ml was the optimal concentration for the gelatinization of collagen. In addition, the PCL scaffolds can provide a topological structure for cells to adhere and migrate, which conventional tissue-engineered corneas cannot. Moreover, PCL/collagen scaffolds have microscale fiber spacing rather than nanoscale spacing of electrospun fibrous scaffolds, which allows the 3D culture of LSSCs [54]. Compared to a conventional structural-free bioengineered cornea, it can be inferred from in vitro experiments that after corneal injury, the activated LSSCs can adhere and migrate along the PCL fibers, and secrete extracellular matrix regularly to repair the corneal defect, so as to reconstruct the normal structure of corneal stroma. The pore of the scaffolds provides space for the growth and differentiation of LSSCs, which also preserves the function of cells to a certain extent and provides the basis for the repair and maintenance of corneal functions, while the traditional corneal replacement fills the corneal defect without retaining the cell function.

3.5 Histological analysis of rat corneal injury treated with PCL/collagen scaffolds in vivo. In our previous studies, we confirmed the mechanical properties and in vitro biocompatibility of PCL scaffolds and PCL/collagen scaffolds. Herein, we assessed the use of a PCL/collagen scaffold specifically designed for corneal stroma wounds in a corneal injury model in Sprague–Dawley rats for the first time. This was done by creating 60% deep corneal defects in SD rats, which was verified by H&E staining (Supplementary Figure S3b). The PCL scaffold and PCL/collagen scaffold were transplanted into wounded corneas through the keratoplasty, and the scaffolds were successfully sutured on corneas. Supplementary Figure S3a and c show the actual and schematic representation of the modeling process.

From the OCT images shown in Figure 4A, the red arrows indicate the positions of the transplanted scaffolds, which can be barely observed because of their thinness. We observed that the corneas exhibited severe edema, and the thickness increased significantly 1 week postoperatively. However, the corneal edema subsided with time, and the thickness of all corneas decreased within 4 weeks. The surface of the cornea became smooth 3 weeks postoperatively, except in the group with corneal damage, and the corneal interior of the two scaffold groups was denser than that in the group with corneal damage due to the regeneration of the corneal stroma. In the experimental group with PCL/collagen scaffold grafts, the corneal morphology gradually became normal within 4 weeks. However, at the end of our observation period, the surface of the cornea in the group with corneal damage was still smooth and the thickness was not uniform.

H&E staining was used to observe the secretion of collagen after corneal injury with different treatments (Figure 4B). In H&E staining, the collagen fibers appeared pale pink [55]. At the early repair stage, collagen secretion was abundant and irregular, accompanied by severe corneal edema and significantly increased corneal thickness. In the middle stage of repair, corneal edema subsided gradually, but the collagen fibers secreted in the repair process were disorganized and without their original morphology and structure, causing corneal fibrosis. Four weeks after repair, with the degradation of rat tail collagen in the scaffold, the remaining collagen fibers were arranged loosely and regularly; thus, the injured cornea treated with PCL/collagen scaffold graft transplantation showed a collagen arrangement most similar to that of the native cornea. Meanwhile, the untreated cornea showed a compact and irregular collagen arrangement. Histological H&E staining revealed that the PCL/collagen scaffold induced the regeneration of the stroma and regularly secreted collagen better than the PCL scaffold.

Collagen distribution and keratocyte differentiation were observed by immunofluorescence staining (Figure 4C). Collagen VI is a unique feature of the extracellular matrix of corneal stromal tissue and is expressed in small amounts in normal corneal tissue (Supplementary Figure S4), secreted by fibroblasts after corneal injury [56]. Collagen is secreted in large quantities and arranged irregularly during the early stages of repair. With the passing of time and the subsidence of corneal edema, the collagen content gradually decreased, and its arranged structure also recovered. This was consistent with the results of the H&E staining. Vimentin is expressed specifically in fibroblasts and is rarely expressed in normal corneas (Supplementary Figure S4) [57, 58]. Thus, we evaluated keratocyte differentiation by observing the expression levels and distribution of vimentin. A large number of fibroblasts differentiated from

keratocytes were observed in injured corneas throughout the whole stromal layer, especially in the early stages of repair. Four weeks after the operation, the fibroblasts and collagen fibers observed in the corneas treated with scaffolds were significantly less than those in the untreated corneas; therefore, we speculated that the scaffold structure could inhibit keratocyte differentiation after injury. Meanwhile, the effect of inhibiting keratocyte differentiation in the PCL/collagen scaffold group was similar to that in the PCL scaffold group, possibly because the fibrous structure inside the collagen slowed down cell adhesion, migration, and transformation, leading to obstruction of cell growth.

Corneal thickness reflected the degree of corneal repair on the other side (Supplementary Figure S5). The corneal edema subsided, and the thickness of all corneas decreased 1 week after surgery. In the next 3 weeks, the thickness of all corneas decreased continually but was still slightly larger than that of the normal rats. Four weeks after repair, there was no significant difference between the thickness of injured corneas treated with PCL/collagen scaffolds and that of the untreated corneas.

Based on the previously mentioned results, the injured corneas treated with PCL/collagen scaffolds achieved ideal outcomes in the restoration of the corneal stromal structure, inhibiting keratocyte differentiation and corneal thickness increase, which is difficult to attain with conventional corneal substitution. Interestingly, we did not add biological factors to the PCL/collagen scaffold, indicating that the repair of the injured cornea depended on the topology of the scaffold. This feature not only helps prevent the immune rejection of the recipient but also makes the production, storage, and transportation of PCL/collagen scaffolds more conducive.

3.6 Related proteins and gene expression assessment of rat corneal injury treated with PCL/collagen scaffolds in vivo. We observed the expression of collagen VI (secreted after injury) and vimentin (specifically expressed in fibroblasts) in the corneas by immunofluorescence staining, and the quantity of collagen VI and vimentin was measured by Western blotting. As shown in Figure 5A and B, vimentin was highly expressed in all corneas in the first week of repair, and there was no significant statistical difference between the experimental groups. At the end of the 4-week observation period, the expression of vimentin in the PCL/collagen scaffold group returned to the normal level, while that of the group with corneal damage was still significantly higher than the normal value. The keratocytes transformed into fibroblasts after injury; nevertheless, the PCL construct inhibited the transformation, and the PCL scaffold infused with collagen showed a superior inhibitory effect.

Collagen is secreted in large quantities to fill the damaged area after corneal injury. However, we found an interesting phenomenon whereby collagen expression was significantly higher in the group with damaged cornea than in the groups treated with scaffold during the first week of repair (Figure 5A, B), which is the critical period for collagen production to repair the defect. Therefore, it is speculated that the scaffold fills the corneal defect area and occupies most of the space, resulting in reduced collagen secretion. The regular arrangement of collagen fibers is a crucial factor in maintaining corneal transparency, which makes it necessary to reduce collagen secretion and guide the regular arrangement of collagen after injury. Various factors have been reported to regulate their bioavailability and function during corneal

wound healing, such as transforming growth factor beta-1 (TGF-β1), TGF-β2, platelet-derived growth factor, and mesenchymal stromal cells (MSCs) [59, 60]. However, for the first time, we found that non-biological scaffolds can also reduce keratocyte differentiation and collagen secretion during repair.

To further verify the effect of scaffolds with special structures on the repair of corneal stromal injury, we used whole-genome sequencing (WGS) and quantitative polymerase chain reaction (qPCR) to characterize the regulation of corneal wound healing. First, we screened out genes that were significantly altered after corneal injury by sequencing the whole genome of normal and injured corneas (Figure 5C, D). In the volcano plot, the x-axis represents the log2 converted multiplier value of difference, and the y-axis represents the -log10 converted significance value. Differentially expressed genes (DEGs) are shown in the volcano plot as dots. Red represents upregulated DEGs, blue represents downregulated DEGs, and gray represents non-DEGs. In the cluster heat map, the horizontal axis represents the log2 of the sample, and the vertical axis represents the gene. The higher the expression level, the closer the color is to red, and on the contrary, the closer the color is to blue. Matrix metalloproteinases (MMPs) are significantly upregulated in injured corneas, which are involved in wound healing processes, including fibrosis [61-63]. Studies have shown that the upregulation of MMPs in diseased corneas is positively associated with levels of corneal neovascularization and fibrosis [64], which makes it meaningful to reduce the degree of MMP upregulation in inhibiting fibrosis. The gene expression of the proliferating cell nuclear antigen (PCNA), which reflects cell proliferation and MMPs, was assessed by qPCR.

From the results shown in Figure 5E, the expression of PCNA was upregulated in all corneas, with the expression being higher in the group with corneal injury, and there was no significant difference between the groups treated with PCL and PCL/collagen scaffolds. This suggested that the quiescent keratocytes were activated and differentiated into fibroblasts after injury, but decreased with time. The groups treated with PCL and PCL/collagen scaffolds showed lower proliferation rates, indicating that the special structure of scaffolds might inhibit the rapid proliferation of cells to a certain extent, which was consistent with the results of previous experiments.

Overexpression of MMPs has been associated with fibrosis in various tissues [65]. As shown in Figure 5F and G, the expression of MMP9 and MMP13 was significantly upregulated in all corneas. The expression of MMP9 showed no significant difference among the three groups in the first week, but the expression of MMP9 in the group treated with PCL/collagen scaffold was lower than that in the other groups at the end of 4 weeks. The expression of MMP13 was similar to that of MMP9. These results indicate that the PCL/collagen scaffold transplanted into injured corneas can minimize the upregulation of MMPs, which can also reduce the transformation of keratocytes into fibroblasts and prevent fibrosis to a certain degree.

4. Conclusions

In summary, we fabricated PCL/collagen scaffolds by direct writing for the first time, showing the capability to reduce the transformation of keratocytes and prevent fibrosis by inhibiting the upregulation of PCNA and MMPs. These scaffolds display a lamellar structure that simulates the native cornea.

Excellent mechanical properties and biocompatibility, as well as regulation of the adhesion and migration of cells to the PCL scaffold fibers, have been demonstrated. We also discovered that the structure of the corneal stromal layer can be restored to the normal level, to the highest possible extent, after treatment of the corneal defect with PCL/collagen scaffold graft transplantation. Moreover, the transformation of keratocytes and the secretion of collagen were also inhibited, which is crucial for preventing fibrosis. This process was fully confirmed by OCT scanning, H&E staining, immunofluorescence staining, Western blot analysis, and qPCR analysis. The reduction of keratocyte differentiation and collagen secretion during repair by PCL/collagen scaffolds without biological factors has been investigated in animal experiments. Using the topological structure of materials to promote wound repair provides a new option for corneal bioengineering and facilitates convenience in the preparation, preservation, and transportation of corneal substitutes. In addition, the advantages of non-immunogenicity and excellent biocompatibility of the PCL/collagen scaffold are highlighted throughout this study, showing a promising application potential in the field of corneal bioengineering.

Abbreviations

CCK-8, Cell Counting Kit-8; DEGs, differentially expressed genes; H&E, hematoxylin and eosin; LSSCs, limbal stromal stem cells; MMPs, matrix metalloproteinases; MSCs, mesenchymal stromal cells; NFES, near-field electrospinning; OCT, optical coherence tomography; PCL, poly(ε-caprolactone); PCNA, proliferating cell nuclear antigen; PEG, poly(ethylene glycol); PFPE, perfluoropolyether; PHEMA, poly(hydroxyethyl methacrylate); PMMA, poly(methyl methacrylate); PVA, poly(vinyl alcohol); qPCR, quantitative polymerase chain reaction; SEM, scanning electron microscope; TGF-β1, transforming growth factor beta-1; WGS, whole-genome sequencing.

Declarations

Declaration of Competing Interest

The authors declare that they have no known competing financial interests or personal relationships that could have appeared to influence the work reported in this paper.

Acknowledgments

This work was financial supported by the National Key Research and Development Program of China (No. 2016YFC1100104 and 2017YFE0103500) and National Natural Science Foundation of China (No.81900912). The authors would like to thank Bin Kong, Shengli Mi(Bio-Manufacturing Engineering Laboratory, Shenzhen International Graduate School, Tsinghua University) for their assistance on this project.

Author Contributions

The manuscript was written through contributions of all authors. All authors have given approval to the final version of the manuscript. [1]These authors contributed equally.

Funding Sources

This work was financially supported by the National Key Research and Development Program of China (No. 2016YFC1100104 and 2017YFE0103500) and the National Natural Science Foundation of China (No. 81900912).

ACKNOWLEDGMENT

The authors would like to thank Bin Kong and Shengli Mi (Bio-Manufacturing Engineering Laboratory, Shenzhen International Graduate School, Tsinghua University) for their assistance with this study.

References

[1] Adil MT, Henry JJ. Understanding cornea epithelial stem cells and stem cell deficiency: Lessons learned using vertebrate model systems. Genesis. 2021: e23411.

[2] Kalha S, Kuony A, Michon F. Corneal epithelial abrasion with ocular burr as a model for cornea wound healing. J Vis Exp. 2018. 137: 58071.

[3] Islam MM, Buznyk O, Reddy JC, et al. Biomaterials-enabled cornea regeneration in patients at high risk for rejection of donor tissue transplantation. NPJ Regen Med. 2018. 3: 2.

[4] Gain P, Jullienne R, He Z, et al. Global survey of corneal transplantation and eye banking. JAMA Ophthalmol. 2016. 134: 167-73.

[5] Whitcher JP, Srinivasan M, Upadhyay MP. Prevention of corneal ulceration in the developing world. Int Ophthalmol Clin. 2002. 42: 71-7.

[6] Bukowiecki A, Hos D, Cursiefen C, Eming SA. Wound-healing studies in cornea and skin: parallels, differences and opportunities. Int J Mol Sci. 2017. 18: 1257

[7] Dunker SL, Armitage WJ, Armitage M, et al. Practice patterns of corneal transplantation in Europe: first report by the European Cornea and Cell Transplantation Registry (ECCTR). J Cataract Refract Surg. 2021.

[8] Avadhanam VS, Smith HE, Liu C. Keratoprostheses for corneal blindness: a review of contemporary devices. Clin Ophthalmol. 2015. 9: 697-720.

[9] Rafat M, Xeroudaki M, Koulikovska M, et al. Composite core-and-skirt collagen hydrogels with differential degradation for corneal therapeutic applications. Biomaterials. 2016. 83: 142-55.

[10] Sweeney DF, Vannas A, Hughes TC, et al. Synthetic corneal inlays. Clin Exp Optom. 2008. 91: 56-66.

[11] Teixeira MA, Amorim M, Felgueiras HP. Poly(vinyl alcohol)-based nanofibrous electrospun scaffolds for tissue engineering applications. Polymers (Basel). 2019. 12:7.

[12] Tamayo Marín JA, Londoño SR, Delgado J, et al. Biocompatible and antimicrobial electrospun membranes based on nanocomposites of chitosan/poly (vinyl alcohol)/graphene oxide. Int J Mol Sci. 2019. 20: 2987.

[13] Orash Mahmoud Salehi A, Nourbakhsh MS, Rafienia M, Baradaran-Rafii A, Heidari Keshel S. Corneal stromal regeneration by hybrid oriented poly (ε-caprolactone)/lyophilized silk fibroin electrospun scaffold. Int J Biol Macromol. 2020. 161: 377-388.

[14] Venkatesan JK, Cai X, Meng W, et al. pNaSS-grafted PCL film-guided rAAV TGF-β gene therapy activates the chondrogenic activities in human bone marrow aspirates. Hum Gene Ther. 2021.

[15] Pallottino F, Figorilli S, Cecchini C, Costa C. Light drones for basic in-field phenotyping and precision farming applications: RGB tools based on image analysis. Methods Mol Biol. 2021. 2264: 269-278.

[16] Fernandes-Cunha GM, Chen KM, Chen F, et al. In situ-forming collagen hydrogel crosslinked via multi-functional PEG as a matrix therapy for corneal defects. Sci Rep. 2020. 10: 16671.

[17] Arica TA, Guzelgulgen M, Yildiz AA, Demir MM. Electrospun GelMA fibers and p(HEMA) matrix composite for corneal tissue engineering. Mater Sci Eng C Mater Biol Appl. 2021. 120: 111720.

[18] Farasatkia A, Kharaziha M, Ashrafizadeh F, Salehi S. Transparent silk/gelatin methacrylate (GelMA) fibrillar film for corneal regeneration. Mater Sci Eng C Mater Biol Appl. 2021. 120: 111744.

[19] Venkatesh P. Vitreous collagen cross-linking and maturation and interactions with internal limiting membrane (ILM) collagen may have a potential role in modulating postnatal growth of the eyeball. Med Hypotheses. 2021. 148: 110519.

[20] Mohammad Siadat S, Silverman AA, DiMarzio CA, Ruberti JW. Measuring collagen fibril diameter with differential interference contrast microscopy. J Struct Biol. 2021: 107697.

[21] Srirampur A, Kola P, Mansoori T, Vemuganti S. Comments on: A comparative study of tarsorrhaphy and amniotic membrane transplantation in the healing of persistent corneal epithelial defects. Indian J Ophthalmol. 2020. 68: 1503-4.

[22] Khalili M, Asadi M, Kahroba H, Soleyman MR, Andre H, Alizadeh E. Corneal endothelium tissue engineering: an evolution of signaling molecules, cells, and scaffolds toward 3D bioprinting and cell sheets. J Cell Physiol. 2020.

[23] Palchesko RN, Carrasquilla SD, Feinberg AW. Natural biomaterials for corneal tissue engineering, repair, and regeneration. Adv Healthc Mater. 2018. 7: e1701434.

[24] Mahdavi SS, Abdekhodaie MJ, Kumar H, Mashayekhan S, Baradaran-Rafii A, Kim K. Stereolithography 3D bioprinting method for fabrication of human corneal stroma equivalent. Ann Biomed Eng. 2020. 48: 1955-70.

[25] Mobaraki M, Soltani M, Zare Harofte S, et al. Biodegradable nanoparticle for cornea drug delivery: focus review. Pharmaceutics. 2020. 12: 1232.

[26] Espana EM, Birk DE. Composition, structure and function of the corneal stroma. Exp Eye Res. 2020. 198: 108137.

[27] Nosrati H, Ashrafi-Dehkordi K, Alizadeh Z, Sanami S, Banitalebi-Dehkordi M. Biopolymer-based scaffolds for corneal stromal regeneration: a review. Polim Med. 2020. 50: 57-64.

[28] Abudhahir M, Saleem A, Paramita P, et al. Polycaprolactone fibrous electrospun scaffolds reinforced with copper doped wollastonite for bone tissue engineering applications. J Biomed Mater Res B Appl Biomater. 2020. 109: 654-64.

[29] Chen HW, Lin MF. Characterization, biocompatibility, and optimization of electrospun SF/PCL/CS composite nanofibers. Polymers (Basel). 2020. 12: 1439.

[30] Kong B, Chen Y, Liu R, et al. Fiber reinforced GelMA hydrogel to induce the regeneration of corneal stroma. Nat Commun. 2020. 11: 1435.

[31] Rabionet M, Yeste M, Puig T, Ciurana J. Electrospinning PCL scaffolds manufacture for three-dimensional breast cancer cell culture. Polymers (Basel). 2017. 9(8): 328.

[32] Li WJ, Tuan RS. Fabrication and application of nanofibrous scaffolds in tissue engineering. Curr Protoc Cell Biol. 2009. Chapter 25: Unit 25.2.

[33] Singh YP, Dasgupta S, Nayar S, Bhaskar R. Optimization of electrospinning process & parameters for producing defect-free chitosan/polyethylene oxide nanofibers for bone tissue engineering. J Biomater Sci Polym Ed. 2020. 31: 781-803.

[34] Anindyajati A, Boughton P, Ruys AJ. Modelling and optimization of polycaprolactone ultrafine-fibres electrospinning process using response surface methodology. Materials (Basel). 2018. 11: 441.

[35] Rafiei M, Jooybar E, Abdekhodaie MJ, Alvi M. Construction of 3D fibrous PCL scaffolds by coaxial electrospinning for protein delivery. Mater Sci Eng C Mater Biol Appl. 2020. 113: 110913.

[36] Park YS, Kim J, Oh JM, et al. Near-field electrospinning for three-dimensional stacked nanoarchitectures with high aspect ratios. Nano Lett. 2020. 20: 441-8.

[37] Turunen S, Joki T, Hiltunen ML, Ihalainen TO, Narkilahti S, Kellomäki M. Direct laser writing of tubular microtowers for 3D culture of human pluripotent stem cell-derived neuronal cells. ACS Appl Mater

Interfaces. 2017. 9: 25717-30.

[38] Alexander FA Jr, Johnson L, Williams K, Packer K. A parameter study for 3D-printing organized nanofibrous collagen scaffolds using direct-write electrospinning. Materials (Basel). 2019. 12: 4131.

[39] Sun X, Yang X, Song W, Ren L. Construction and evaluation of collagen-based corneal grafts using polycaprolactone to improve tension stress. ACS Omega. 2020. 5: 674-82.

[40] Nazir R, Bruyneel A, Carr C, Czernuszka J. Collagen type I and hyaluronic acid based hybrid scaffolds for heart valve tissue engineering. Biopolymers. 2019. 110: e23278.

[41] Sun X, Wang J, Wang Y, Zhang Q. Collagen-based porous scaffolds containing PLGA microspheres for controlled kartogenin release in cartilage tissue engineering. Artif Cells Nanomed Biotechnol. 2018. 46: 1957-66.

[42] She Y, Fan Z, Wang L, et al. 3D printed biomimetic PCL scaffold as framework interspersed with collagen for long segment tracheal replacement. Front Cell Dev Biol. 2021. 9: 629796.

[43] Zhang H, Pei Z, Wang C, Li M, Zhang H, Qu J. Electrohydrodynamic 3D printing scaffolds for repair of Achilles tendon defect in rats. Tissue Eng Part A. 2021.

[44] Wang J, Sun X, Zhang Z, et al. Silk fibroin/collagen/hyaluronic acid scaffold incorporating pilose antler polypeptides microspheres for cartilage tissue engineering. Mater Sci Eng C Mater Biol Appl. 2019. 94: 35-44.

[45] Ma L, Yu Y, Liu H, et al. Berberine-releasing electrospun scaffold induces osteogenic differentiation of DPSCs and accelerates bone repair. Sci Rep. 2021. 11: 1027.

[46] Vonbrunn E, Mueller M, Pichlsberger M, et al. Electrospun PCL/PLA scaffolds are more suitable carriers of placental mesenchymal stromal cells than collagen/elastin scaffolds and prevent wound contraction in a mouse model of wound healing. Front Bioeng Biotechnol. 2020. 8: 604123.

[47] Sanie-Jahromi F, Eghtedari M, Mirzaei E, et al. Propagation of limbal stem cells on polycaprolactone and polycaprolactone/gelatin fibrous scaffolds and transplantation in animal model. Bioimpacts. 2020. 10: 45-54.

[48] Fernández-Pérez J, Kador KE, Lynch AP, Ahearne M. Characterization of extracellular matrix modified poly(ε-caprolactone) electrospun scaffolds with differing fiber orientations for corneal stroma regeneration. Mater Sci Eng C Mater Biol Appl. 2020. 108: 110415.

[49] Brown TD, Dalton PD, Hutmacher DW. Direct writing by way of melt electrospinning. Adv Mater. 2011. 23: 5651-7.

[50] He FL, Li DW, He J, et al. A novel layer-structured scaffold with large pore sizes suitable for 3D cell culture prepared by near-field electrospinning. Mater Sci Eng C Mater Biol Appl. 2018. 86: 18-27.

[51] Wu J, Du Y, Watkins SC, Funderburgh JL, Wagner WR. The engineering of organized human corneal tissue through the spatial guidance of corneal stromal stem cells. Biomaterials. 2012. 33: 1343-52.

[52] Kilic Bektas C, Hasirci V. Mimicking corneal stroma using keratocyte-loaded photopolymerizable methacrylated gelatin hydrogels. J Tissue Eng Regen Med. 2018. 12: e1899-e1910.

[53] van den Berg TJ, Tan KE. Light transmittance of the human cornea from 320 to 700 nm for different ages. Vision Res. 1994. 34: 1453-6.

[54] Rahmati Nejad M, Yousefzadeh M, Solouk A. Electrospun PET/PCL small diameter nanofibrous conduit for biomedical application. Mater Sci Eng C Mater Biol Appl. 2020. 110: 110692.

[55] Feldman AT, Wolfe D. Tissue processing and hematoxylin and eosin staining. Methods Mol Biol. 2014. 1180: 31-43.

[56] Schlötzer-Schrehardt U, Bachmann BO, Tourtas T, et al. Ultrastructure of the posterior corneal stroma. Ophthalmology. 2015. 122: 693-9.

[57] Wilson SL, El Haj AJ, Yang Y. Control of scar tissue formation in the cornea: strategies in clinical and corneal tissue engineering. J Funct Biomater. 2012. 3: 642-87.

[58] Funderburgh JL, Mann MM, Funderburgh ML. Keratocyte phenotype mediates proteoglycan structure: a role for fibroblasts in corneal fibrosis. J Biol Chem. 2003. 278: 45629-37.

[59] de Oliveira RC, Tye G, Sampaio LP, et al. TGFβ1 and TGFβ2 proteins in corneas with and without stromal fibrosis: delayed regeneration of apical epithelial growth factor barrier and the epithelial basement membrane in corneas with stromal fibrosis. Exp Eye Res. 2021. 202: 108325.

[60] Samaeekia R, Rabiee B, Putra I, et al. Effect of human corneal mesenchymal stromal cell-derived exosomes on corneal epithelial wound healing. Invest Ophthalmol Vis Sci. 2018. 59: 5194-200.

[61] Gao N, Liu X, Wu J, et al. CXCL10 suppression of hem- and lymph-angiogenesis in inflamed corneas through MMP13. Angiogenesis. 2017. 20: 505-18.

[62] Ma J, Zhou D, Fan M, et al. Keratocytes create stromal spaces to promote corneal neovascularization via MMP13 expression. Invest Ophthalmol Vis Sci. 2014. 55: 6691-703.

[63] Wang X, Tang L, Zhang Z, Li W, Chen Y. Keratocytes promote corneal neovascularization through VEGFr3 induced by PPARα-inhibition. Exp Eye Res. 2020. 193: 107982.

[64] Wolf M, Clay SM, Oldenburg CE, Rose-Nussbaumer J, Hwang DG, Chan MF. Overexpression of MMPs in corneas requiring penetrating and deep anterior lamellar keratoplasty. Invest Ophthalmol Vis Sci. 2019.

60: 1734-47.

[65] Chuang HM, Chen YS, Harn HJ. The versatile role of matrix metalloproteinase for the diverse results of fibrosis treatment. Molecules. 2019. 24: 4188.

Figures

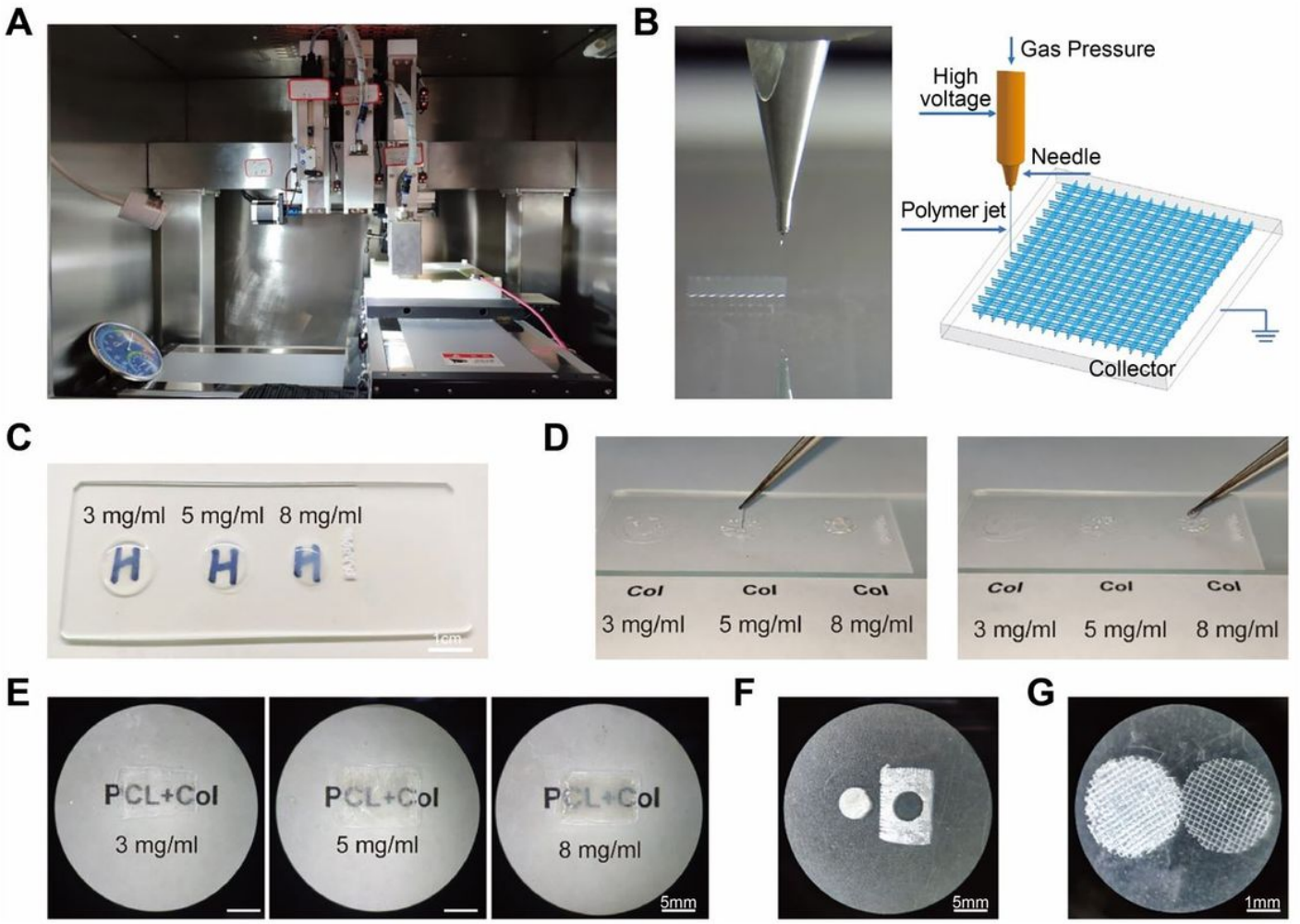

Figure 1

Preparation of the PCL/collagen scaffold. (A) The actual direct writing device. (B) The actual and schematic representation of the Taylor cone, which ejects a polymer jet. (C) The macroscopic morphology of collagen at 3-mg/ml, 5-mg/ml, and 8-mg/ml concentrations. The scale bar is 1 cm. (D) The gelatinization of collagen with 5-mg/ml and 8-mg/ml concentrations. (E) The microscopic morphology of the PCL/collagen scaffolds with 3-mg/ml, 5-mg/ml, and 8-mg/ml concentrations. The scale bars are 5 mm. (F) The corneal graft was cut from a rectangular scaffold with a 3.25-mm-diameter trephine. The scale bar is 5 mm. (G) The microscopic morphology of the PCL scaffold and PCL/collagen scaffold. The scale bar is 1 mm.

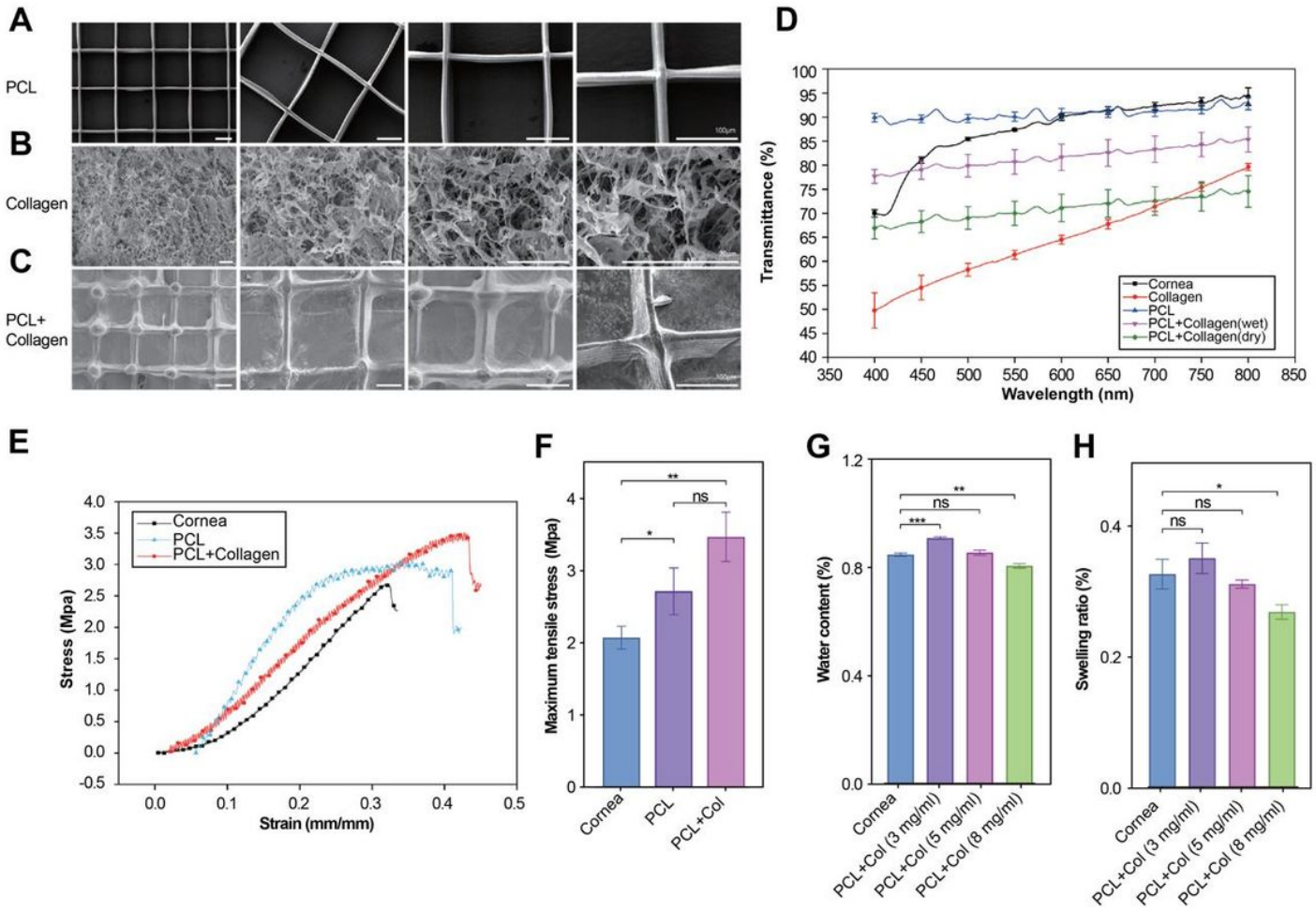

Figure 2

Physical characterization of the PCL/collagen scaffold. (A, C) Scanning electron microscope (SEM) images of the PCL scaffold and the PCL/collagen scaffold under different magnifications (200×, 400×, 800×, and 1500×). The scale bars represent 100 μm. (B) SEM images of rat tail collagen type I at 5-mg/ml concentration under different magnifications (800×, 2000×, 3000×, and 6000×). The scale bars represent 20 μm. (D, E, F) The transmittance, strain–stress curves, and maximum tensile stress of the PCL scaffold, PCL/collagen scaffold, and cornea. (G, H) The water content and swelling ratio of the cornea and PCL scaffolds infused with collagen at 3-mg/ml, 5-mg/ml and 8-mg/ml concentrations. The error bars indicate means ± SD and n = 3: *p < 0.05, **p <0.01, ***p <0.001.

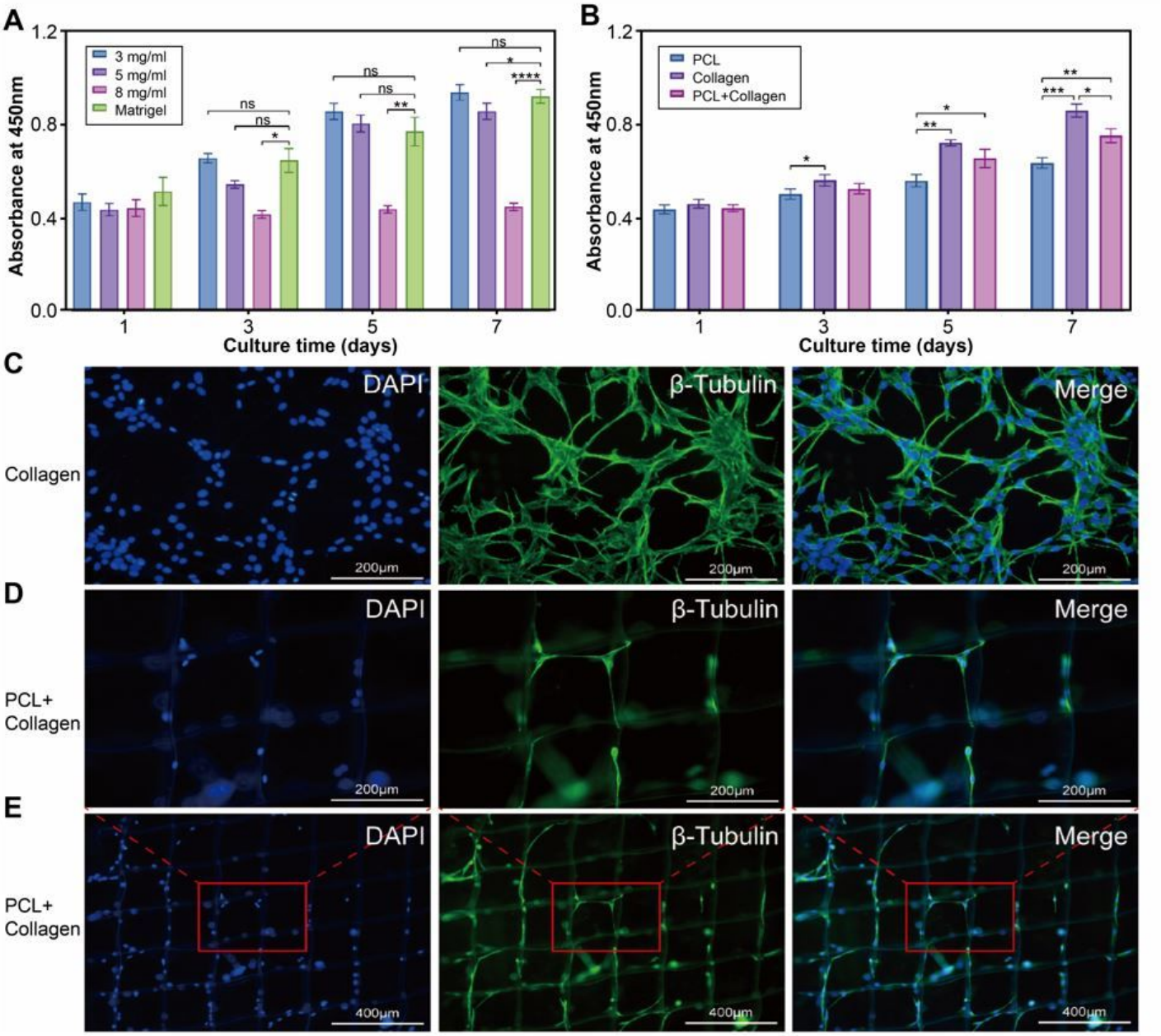

Figure 3

Biocompatibility of the PCL/collagen scaffold in vitro. (A) Cell proliferation of Matrigel and collagen at concentrations of 3 mg/ml, 5 mg/ml, and 8 mg/ml for day 1, 3, 5, and 7. (B) Cell proliferation of PCL scaffolds, collagen, and PCL/collagen scaffolds for day 1, 3, 5, and 7. (C, D, E) β-Tubulin expression staining of LSSCs in collagen and PCL/collagen scaffold after culturing for 3 days. The scale bars of C and D are 200 μm. The scale bars of E are 400 μm. The error bars indicate means ± SD and n = 3: *p < 0.05, **p <0.01, ***p <0.001, ****p <0.0001.

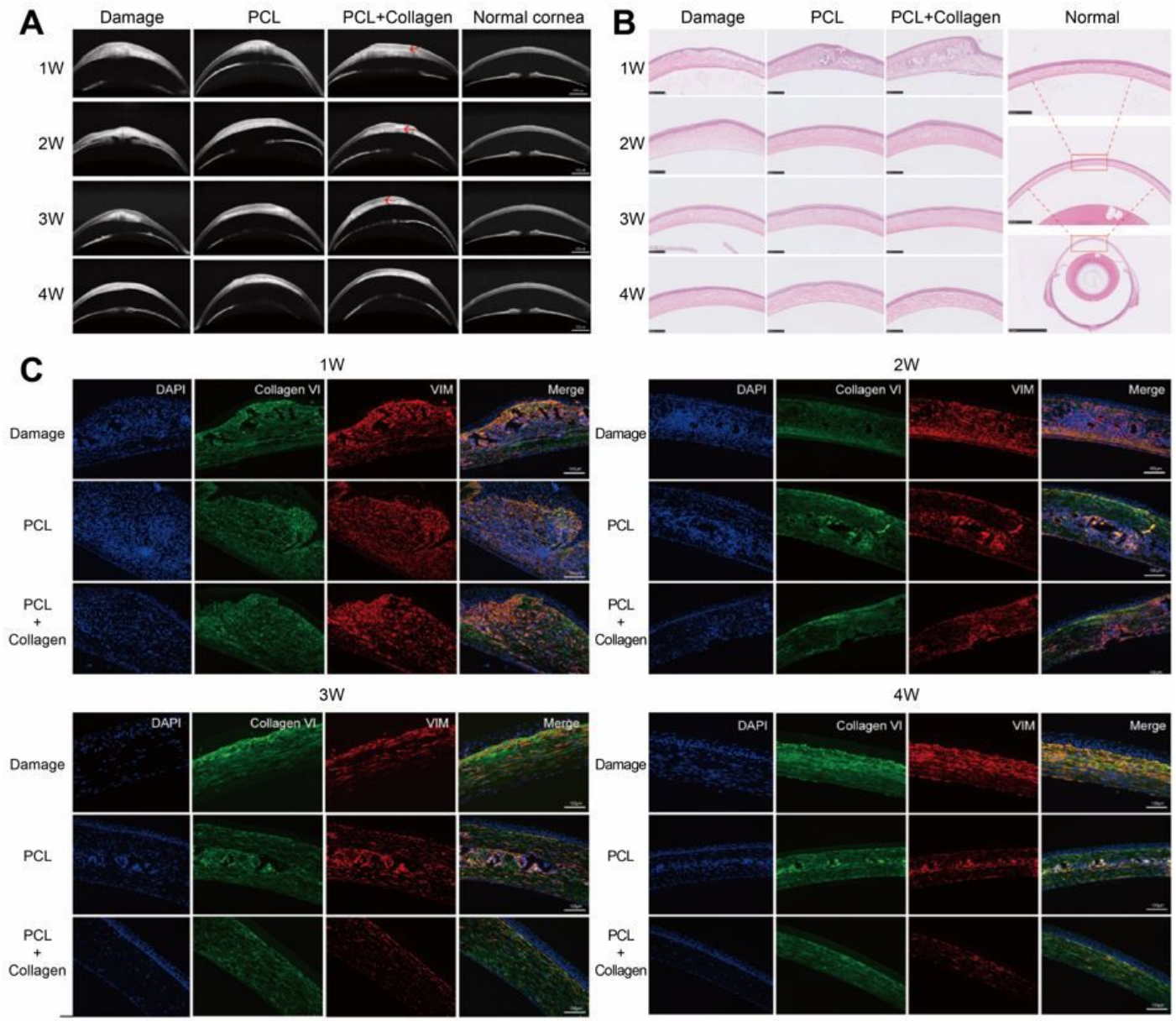

Figure 4

Histological analysis. (A) Optical coherence tomography (OCT) images of the postoperative corneas at each week. The red arrows indicate the position of the scaffolds. The scale bar is 500 μm. (B) Hematoxylin and eosin (H&E) staining of the postoperative corneas at each week; the scale bar is 250 μm. (C) Immunofluorescence staining images of different groups after operation at each week. Green represents collagen type VI, red represents vimentin, and blue represents nuclei.

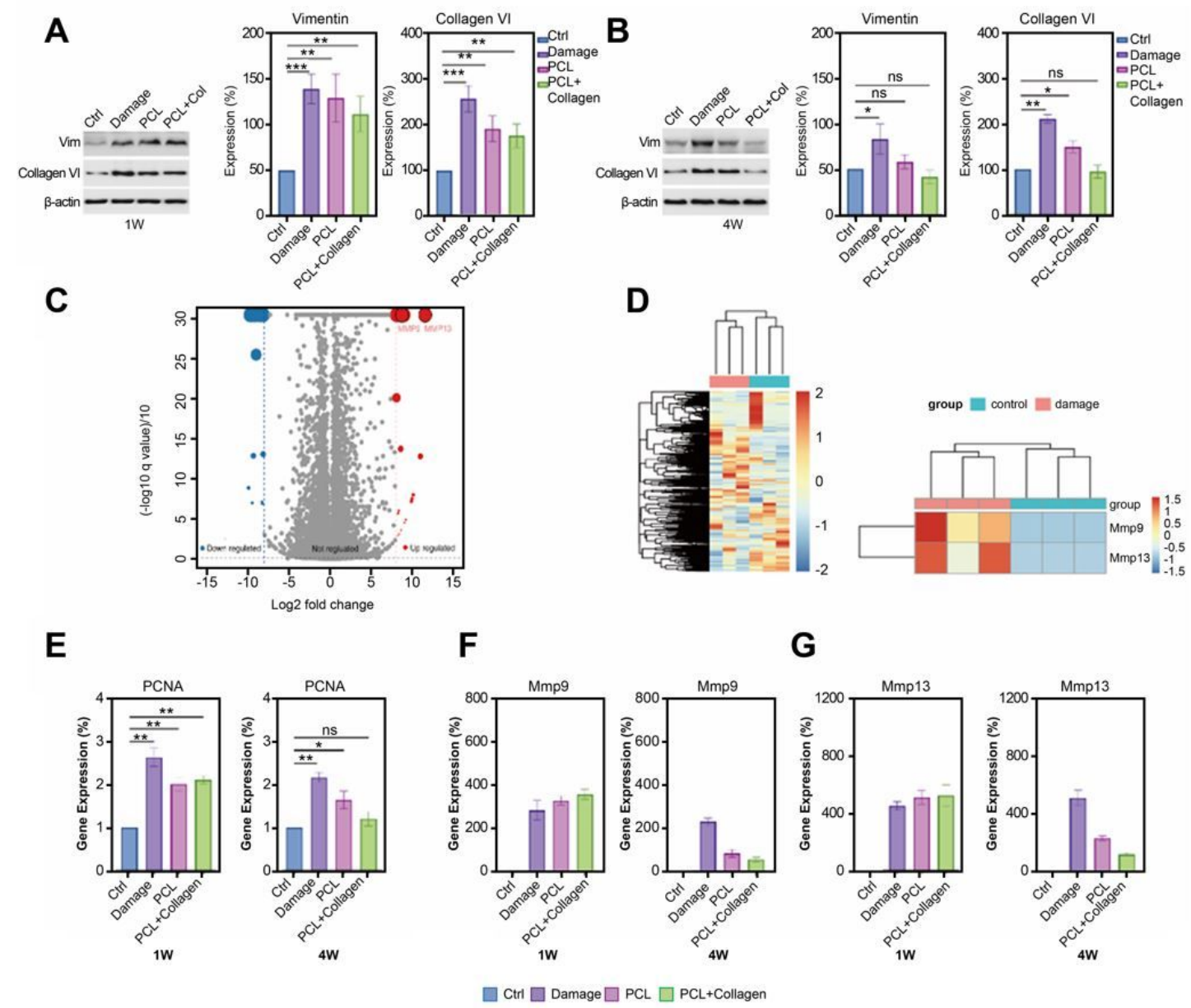

Figure 5

Related proteins and gene expression assessment. (A, B) Western blot test and statistical results of vimentin and collagen type VI of the different groups. (C, D) Volcano plot and heat map of the whole-genome sequencing of normal cornea and damaged cornea. (E, F, G) Gene expression and statistical results of proliferating cell nuclear antigen, MMP9, and MMP13 in different groups. The error bars indicate means ± SD and n = 3: *p < 0.05, **p <0.01, ***p <0.001.

Supplementary Files

This is a list of supplementary files associated with this preprint. Click to download.

- NanoSupplementarymaterialsandmethods.docx
- OnlineSF1.png
- OnlineSF2.png
- OnlineSF3.png
- OnlineSF4.png
- OnlineSF5.png
- scheme1.jpg